A Platform for Grasp Performance Assessment in Compliant or Underactuated Hands

Gert A. Kragten[1]
e-mail: g.a.kragten@tudelft.nl

Just L. Herder
e-mail: j.l.herder@tudelft.nl

Department of BioMechanical Engineering,
Faculty of Mechanical, Maritime and Materials Engineering,
Delft University of Technology,
Mekelweg 2,
2628 CD Delft, The Netherlands

This paper presents the design and evaluation of a platform for the assessment of the performance of compliant or underactuated hands. The position of objects relative to the hand can be varied in order to assess the successful grasp region. The boundary positions of this region can be measured with a precision of 3 mm. In addition, the force required to pull an object all the way out of the hand from a stable initial configuration is measured with a precision of 0.2 N for frictionless grasping. These experiments are proposed as benchmark tests to quantify the functional performance of compliant or underactuated robotic hands. This platform considers planar symmetrical grasps, where objects can move along the line of symmetry. An innovative approach to emulate frictionless grasps of circular objects is proposed as well.
[DOI: 10.1115/1.4000761]

1 Introduction

Underactuation in robotic hands seems a promising approach to grasping a variety of objects without a very complex mechanical system and control architecture [1]. Underactuated hands have fewer actuators than degrees of freedom (DoF), and can therefore intrinsically adapt to the shape of the objects. Consequently, the closing motion of the fingers, and the contact forces that the fingers apply to the objects, are not fully controllable. This implies that the grasp performance is mainly determined by the mechanical design and must be considered at an early design stage.

An unambiguously defined grasp performance metric for robotic hands does not exist. Consequently, there is no uniformity in the way that grasp performance is calculated or measured. The grasp performance is conventionally quantified by the grasp stability (i.e., the ability to resist position disturbances on the object) or by form and force closure properties (i.e., the ability to resist force disturbances on the object) [2]. In these quantifications, independent control of all phalanges is assumed to determine the stability or closure type. However, underactuated hands do not have independent control. Many alternative performance metrics were therefore applied at the design and evaluation stage of underactuated hands, including the following.

1. In Ref. [3], the closing motion of the fingers was optimized to mimic the motion human fingers.
2. Isotropy of the normal contact forces applied to the objects was considered in the design and evaluation of, for example, the Soft Gripper [4]. Isotropy of the contact forces was tested by observation of the indention of a particular soft object at the contact points.
3. In Refs. [5,6], the ability to apply (compressive) contact forces with all the phalanges of underactuated fingers was studied and applied to the design of linkage driven and cable-pulley driven fingers.
4. The SDM hand [7] was optimized, considering the ability to envelope objects and considering the resultant of the contact forces on the object. A platform was built where the ability to envelope cylindrical objects of different sizes was observed, and where the resultant contact force on the objects was measured.
5. Kamikawa and Maeno [8] tested the force needed to pull objects out of their underactuated hand, while a different performance criterion was used to optimize the design.

An extended overview of performance metrics applied at the design and evaluation stage can be found in Ref. [9]. That overview also showed that the number of prototypes that are evaluated by structured experiments is very limited. Platforms to measure performance hardly exist. Since comparison of the performance of different underactuated hands is currently almost impossible, feasible directions for fundamental improvements in the design of underactuated grasping remain unknown.

In Refs. [9,10], the ability to grasp and to hold objects with underactuated hands was quantified, based on a benchmark proposal of the European Robotics Research Network (EURON) [11]. The ability to grasp means being able to achieve stable equilibrium of freely moving objects by just using the fingers (and palm) of the hand. The ability to hold means being able to keep the grasped objects in the hand while disturbing forces are applied to the objects. In Ref. [9], a static model was proposed to calculate these performance metrics as a function of the design parameters. This model used cylindrical objects moving in a plane, and lets the underactuated fingers passively reconfigure to find a grasp equilibrium or to resist force disturbances on the object. Rigid, frictionless contact between the object and fingers, as well as soft, frictional contact were modeled [12]. However, the possibility to measure the ability to grasp and to hold objects, and the validity of the grasp model has not been demonstrated yet by extensive experiments.

The objective of this paper is to present the design of a platform to experimentally assess the ability to grasp and hold various objects by compliant or underactuated hands. The platform will be technically evaluated using a specific underactuated finger mechanism. Preliminary results of performance experiments with this platform will be shown. To simplify the experiments, the platform is created to assess planar, symmetrical grasps perpendicular to the gravity field, while cylindrical objects are pulled out of the hand along the line of symmetry. An emulation of a frictionless object is created in order to verify the theoretical results of grasp models that assume frictionless contact points between the object and the fingers.

The main contribution of this new platform is the assessment of the ability of underactuated hands to grasp a range of objects and to resist disturbing forces by relatively simple measurements. Such measurements are important to quantify the performance of an underactuated hand and to compare these values with measurements executed with other underactuated hands. In addition, the platform enables the validation of grasp models—for the first time, even those that assume zero friction between object and fingers—by comparing the theoretically expected performance with the experimental results.

2 Design Specifications

The objective of the platform was to assess the ability to grasp and to hold objects as a function of design parameters of compli-

[1]Corresponding author.

Contributed by the Design Automation Committee of ASME for publication in the JOURNAL OF MECHANICAL DESIGN. Manuscript received February 2, 2009; final manuscript received November 17, 2009; published online January 20, 2010. Assoc. Editor: Matthew B. Parkinson.

ant or underactuated hands. Such a hand can be represented by a single finger because of the limitations to consider only planar, symmetrical grasp cases where objects only move along the line of symmetry. To investigate the effect of changing the mechanical design of the fingers on the performance, criteria on the precision of the experiments are specified in this section. Precision is expressed here as two times the standard deviation (2σ) of the measured parameter.

To assess the ability to grasp, objects of various sizes had to freely move on the line of symmetry, while the finger encloses the object. The farthest initial position of the object was assumed to be less than a finger length away from the palm. The finger length was chosen to be 160 mm, based on a 2:1 scale of a human finger. It was desired to measure the initial position of the object for which the finger was able to obtain grasp equilibrium, as well as the final equilibrium position with a precision of 3 mm ($<2\%$ of the full scale). In our opinion, more precise measurements were not realistic because of frictional effects between the object and the fingers.

To assess the ability to hold, cylindrical objects were pulled at a low but constant velocity of about 2 mm/s out of the hand. The pull force was measured as a function of object position. The maximum force to pull the object was assumed to be less than 5 N, while the maximum displacement had to be about 1.2 times the finger length. It was decided to measure this pull force as a function of the object position with a precision of 0.1 N (2% of the maximum force) and the position with a precision of 1 mm. For both types of experiments, the diameter of the object had to be easily adjustable.

The design parameters, which were expected to have the strongest influence on the performance, were the relative joint stiffnesses, the distance between the proximal joints of the fingers, and the friction between the fingers and the object. Hence, easy adaptation of these design parameters was required. In addition, experiments with grasps of zero friction between the object and fingers had to be realized.

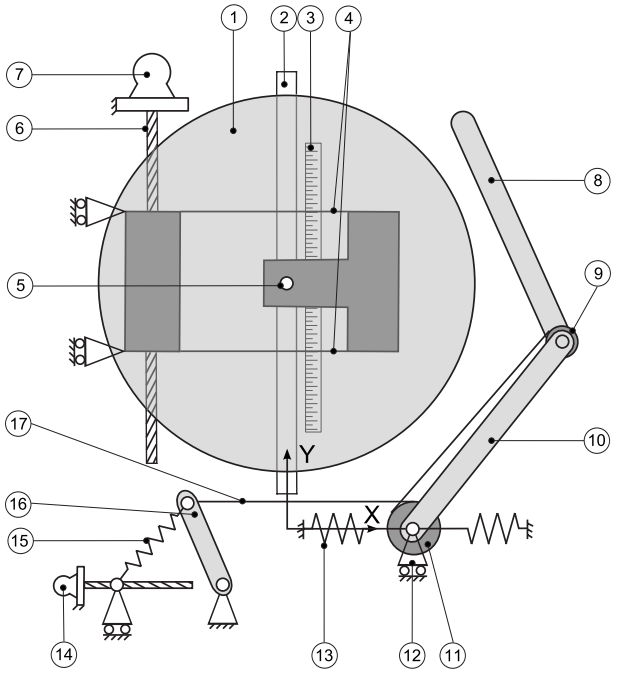

Fig. 1 Schematic overview of the main components of the platform. The numbering of the components corresponds with the numbering in Figs. 2–6. (1) is an object; (2–3) are components to let the object freely move, see Fig. 2; (4–7) are components to pull the object out of the hand and measure the required force, see Figs. 3 and 4; (8–13) are components belonging to the underactuated finger, see Fig. 5; and (14–17) are components to actuate the finger with a constant force, see Fig. 6. *X* and *Y* are the axes of the global reference frame.

3 Conceptual and Dimensional Design

This section addresses the design of the three main components of the platform. First, the design of a freely moving object that emulates a frictionless object is addressed. Then, the components to measure the force needed to displace objects all the way out of the hand are described. Finally, the dimensional design of an adjustable, underactuated finger is shown. A schematic drawing of these three components is shown in Fig. 1.

3.1 Freely Moving, Frictionless Objects. For the validation of zero friction models on the platform, we propose cylindrical objects consisting of acrylic disks of the same diameter, as shown in Fig. 2. These disks are supported by miniature deep groove ball bearings with low friction (SKF, 618/4, nominal frictional moment is smaller than 0.050 N mm) and can rotate independently about a vertical axis. There are as many disks as there are phalanges. Each disk makes contact with one phalanx only. When the object moves with respect to the finger, the disks are thus rolling over the phalanges instead of sliding. The small friction moment in the ball bearings of the rolling object hardly affects the contact forces on the object surface, because the diameter of the object is ten times larger than the diameter of the bearings. Consequently, these objects are kinematically and kinetically equivalent to objects that slide without friction along the contact areas of the phalanges. For experiments with friction at the contact points, cylindrical objects that could not rotate about the vertical axis were created.

For the experiments assessing the ability to grasp, free movement of objects on the line of symmetry (i.e., *Y*-axis in Fig. 1) had to be constructed. Accepting some friction in this line of motion, we decided to use a linear guide (THK, RSR9KM), on which the central axis of the objects can be fixed by a bolt. A ruler with a scale division of 0.5 mm was placed along the linear guide to visually determine the initial and final position of the object with respect to the global reference frame. The minimal and maximal distance of the center of the object on this guide is 35 mm and 190 mm, respectively.

3.2 Pull Force—Displacement Experiment. For the experiments measuring the force required to completely pull an object out of the hand (i.e., the ability to hold), a lead screw (Kerk,

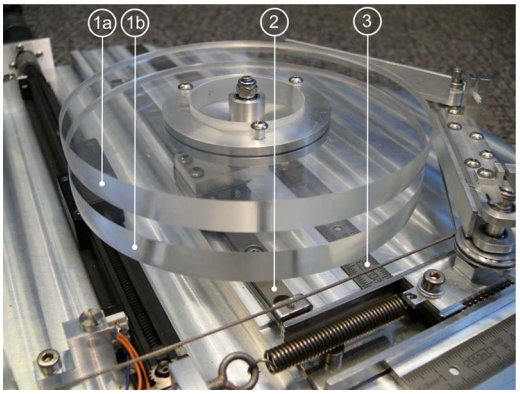

Fig. 2 Picture of a freely moving object consisting of two independently rotating disks to assess frictionless grasping, where (1a) is the upper disk in contact with the distal phalanx; (1b) is the lower disk in contact with the proximal phalanx; (2) is the linear guide; and (3) is the ruler to measure the initial and final position of the object. The underactuated finger is visible at the right side of the picture.

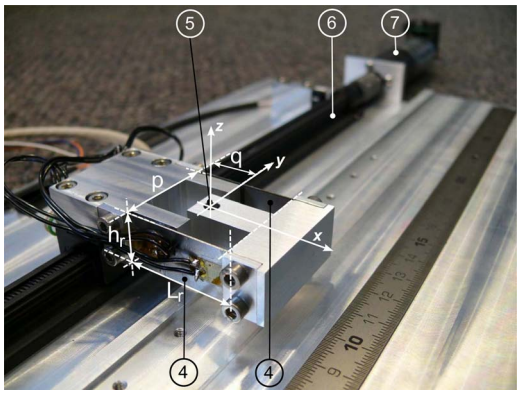

Fig. 3 Load cell based on a straight line guidance with leaf springs, where (4) are leaf springs of thickness t, length L_r, and height h_r mounted on a distance p, according Table 1; (5) is the hole in the slider where the shaft of the object is mounted on a distance $q=L_r/2$ from the base; (6) is the lead screw; and (7) is the DC-motor

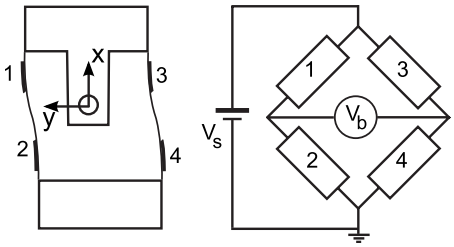

Fig. 4 Schematic drawing of the top view of the load cell (left side) and Wheatstone's bridge configuration (right side) with the four strain gauges (1, 2, 3, and 4), supply voltage V_s, and voltage across the bridge V_b

RGS4010, pitch 0.1″) actuated by a DC-motor (Maxon, A-max26, gear GP26 81:1, and encoder Enc22) was applied to move the object along the line of symmetry by a constant, low velocity. To obtain a constant velocity, a servoamplifier (Maxon, LSC30/2) was used in its Encoder mode.

To measure the force needed to displace the object, a specially made load cell was mounted between the object and the nut of the lead screw, as shown in Fig. 3. Measuring friction in the system that supported and actuated the object was thus avoided. The main forces and moments on the load cell are caused by the contact forces of the finger on the object parallel to the X,Y-plane, as well as the weight of the object in the perpendicular direction. To only measure forces in the direction of the displacement (Y-axis), the construction of the load cell was based on a straight line guidance with two parallel leaf springs with dimensions, as shown in Table 1. Such a mechanism is stiff in all directions, except the direction perpendicular to the leaf springs. Four strain gauges (HBM, 1-LY41–3/350) were glued to the leaf springs and electrically connected in a full Wheatstone's bridge configuration, according to Fig. 4, where the voltage across the bridge is amplified (Scaime, CPJ). For this bridge configuration, only the strain due to bending of the leaf springs caused by sideways displacement results in a potential difference across the bridge, while strain due to normal compression or tension does not result in a potential difference. Ideally, only the forces due to displacements of the object along the line of symmetry are thus measured.

3.3 Adjustable, Underactuated Finger. It was decided to initially create one specific finger inspired by the mechanism of the Soft Gripper [4], as it is already well described in the literature. The fingers of this gripper consist of ten independently rotating phalanges driven by a cable routed via pulleys of decreasing diameter. As opposed to the Soft Gripper, a finger with only two phalanges was created. In addition, an extra compliant DoF at the proximal joint was added in order to passively adjust the distance between the finger and line of symmetry, as shown in Figs. 1 and 5. This extra compliant DoF is constructed by a low-friction linear guide (THK, ER1025), while preloaded springs at both sides of the slider provide the desired stiffness and initial position. The dimensions of the finger were based on a 2:1 scale of the human finger, resulting in dimensions, as shown in Table 2.

The stiffness and initial angle of the revolute joints can be discretely adjusted by replacing the torsional springs, which are mounted in the joints of the phalanges (see Fig. 5). The stiffness of the prismatic joint can be adjusted similarly. The attachment points of the linear springs with the fixed world can be moved by a threaded bar in order to vary the initial position of the finger with respect to the line of symmetry. The minimal and maximal position of the finger with respect to the line of symmetry is 41 mm and 98 mm, respectively. The contact material on the phalanges can be changed by replacing the contact surfaces. These surfaces are mounted to the finger by two, directly accessible, socket head screws.

The finger is mechanically actuated by a cable tensioned by a constant force irrespective of the configuration of the finger. Given the dimensions of the finger in Table 2 and a maximum

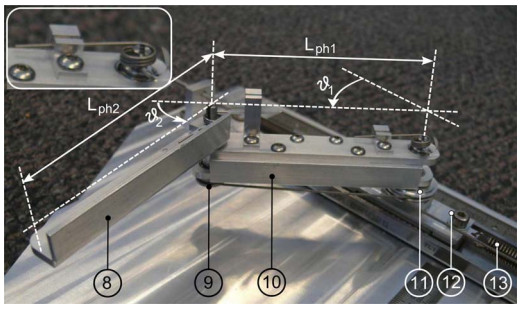

Fig. 5 Underactuated finger mechanism, where (8) is the contact area of the distal phalanx of length L_{ph_2} and with rotation ϑ_2 with respect to the proximal phalanx; (9) is the distal pulley; (10) is the contact area of the proximal phalanx of length L_{ph_1} and with rotation ϑ_1 with respect to the prismatic joint; (11) is the proximal pulley; (12) is the slider of the prismatic joint; (13) is a linear spring for preloading the prismatic joint. In the upper left corner, a detail of the torsional spring at the proximal joint is shown.

Table 1 Main dimensions of the load cell

Dimensions	Explanation
L_r (30.0 mm)	Length of leaf springs
h_r (15.0 mm)	Height of leaf springs
t (0.4 mm)	Thickness of leaf springs
p (28.0 mm)	Distance between leaf springs
q (15.0 mm)	Distance from base where forces apply

Table 2 Main dimensions of the underactuated finger

Dimensions	Explanation
L_{ph} (80.0 mm)	Length of contact area of phalanges
h_{ph} (10.0 mm)	Height of contact area of phalanges
r_1 (9.95 mm)	Radius proximal pulley
r_2 (4.80 mm)	Radius distal pulley

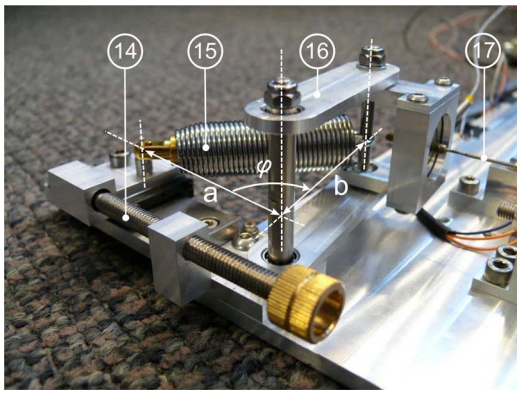

Fig. 6 Constant force actuator, where (14) is the screw to adjust length *a*; (15) is the nearly zero-free-length spring generating a force F_s; (16) is the lever arm of length *b*=50 mm and rotation angle φ; and (17) is the actuation cable that applies a force F_a on the finger

pulling force of 5 N, the magnitude of the actuation force had to be approximately 20 N according to simulations with the grasp model. It was chosen to not obtain this constant force by using a dead weight because of the disproportional inertia increase in the system. Instead, we constructed a lever arm, as shown in Fig. 6, which was preloaded by a nearly zero-free-length spring. The spring force of a perfect zero-free-length spring is proportional to its length

$$F_s = k_s L_s \tag{1}$$

where F_s is the spring force, k_s is the spring stiffness, and L_s is the actual length of the spring. With such a spring, the force in the cable is constant, irrespective of the rotation of the lever, according to the following equation based on the moment balance around point O_s [13]:

$$F_a b \sin\varphi = F_s b \frac{a \sin\varphi}{L_s} \tag{2}$$

$$F_a = k_s a \tag{3}$$

where F_a is the actuation force in the cable that drives the finger, b is the length of the lever arm (50 mm), a is an adjustable length between the joint of the lever arm and the attachment of the spring with the fixed world, φ is the rotation angle of the lever arm, and L_s can be determined by the cosine rule. On this platform, the spring does not have a perfect zero-free-length, but a small negative free length

$$F_s = 0.37 L_s - 1.89 \tag{4}$$

φ is expected to vary between $(4/9)\pi < \varphi < (5/9)\pi$ during the experiments. When a is adjusted to, for example, 64 mm, the actuation force is thus not perfectly constant, but equal to $F_a = 22.15 \pm 0.15$ N, based on Eqs. (2) and (4).

To enclose the finger around the object, the adjustment screw of the actuator is manually tightened, which increases the tension in the cable from initially an almost zero force to the desired actuation force. The actual cable force is measured by a force sensor (Futek, LTH300) and amplified (Futek, CSG110).

3.4 Data Acquisition. The output voltages from the amplifiers of the force sensor of the actuation cable and the load cell were collected at a sample rate of about 100 Hz with a USB-DAQ (National Instruments, USB-6009) and using LABVIEW 8.2 on a standard PC. The position of the object on the lead screw during the experiments was postcalculated, based on the recorded time, and knowing the initial position and constant velocity of the object. For data interpretation and visualization, standard routines in MATLAB were used.

Table 3 Sensitivity analysis of the load cell in V/N. In all load cases, a high linearity was obtained ($R^2 > 0.99$, where R is Pearson's correlation coefficient).

Load case	1	2	3	4	5
Sensitivity (V/N)	<0.005	<0.005	1.10	1.11	1.11

4 Evaluation and Preliminary Experimental Results

4.1 Evaluation of Platform Components. In this section, the friction in the linear guides, the constant velocity actuation of the object, the sensitivity of the load cell, and the precision of the constant force actuator are addressed.

The friction in the linear guides of the platform was measured by pivoting the rail at one end from a horizontal to an inclined configuration, and measuring the inclination angle at which the slider started to move downward. The sine of this angle, multiplied by the weight of the slider (and if applicable a mounted object), resulted in the friction force of the slider with the rail. This measurement was repeated ten times ($N=10$) because of the observed variance during pilot measurements. The friction in the prismatic joint of the underactuated finger was measured to be 0.07 N ($\sigma=0.02$ N). The friction in the linear guide used for the grasping experiment was measured to be 0.14 N ($\sigma=0.02$ N), while it was loaded with an object weighing 0.346 kg. A normal distribution of the repeated measurements was demonstrated by a Kolmogorov–Smirnov test. The revolute joints are provided with deep groove ball bearings (SKF, 618/4). According to the specifications, the rotational friction should be less than 0.050 N mm in nominal loading cases, which can be neglected.

The mean constant velocity of the object was 1.765 mm/s ($\sigma = 2.0 \times 10^{-3}$ mm/s) over the full length of the lead screw with the current settings of the servoamplifier. This velocity was determined by repeated measurements in an unloaded ($N=5$) and loaded ($N=5$) case. In the loaded case, a force of 2 N was applied to the nut of the lead screw, oppositely directed with respect to the velocity. The minimal and maximal distance of the center of the object on the lead screw with respect to the palm of the hand is 44 mm and 230 mm, respectively. Hence, using 2σ as confidence interval, the precision of the measured position at the end of the lead screw is 0.5 mm.

The load cell to measure the displacement force on the object was calibrated for the following five load cases: (1) forces parallel to the leaf springs (along negative x-axis), applied at the center of the load cell; (2) forces along the negative x-axis, applied at an offset of 39 mm in positive z-direction; (3) forces along the y-axis, applied at O_{LC}; (4) forces along the y-axis, applied at an offset of 39 mm in positive z-direction; (5) forces along the y-axis, applied at an offset of 110 mm in the positive x-direction (x, y, and z were shown in Fig. 3). These offsets were applied to investigate the sensitivity of the load cell for bending moments. The maximally applied force was 10 N in load cases (1–2), and 5 N in cases (3–5). The input voltage on the bridge circuit was 24.0 V. The sensitivity of the load cell for all these load cases are shown in Table 3. During experiments, a combination of case (2, 4, and 5) will apply on the load cell, while ideally, only case (3) would apply. Consequently, the worst case systematic error of the measured pulling force can be +0.1 N.

We experimentally determined the variation in the actual actuation force in the relevant range of motion. With the screw adjusted at $a=64$ mm, the actuation force could vary between minimal $F_a=20.8$ N (at $\varphi=(4/9)\pi$) and maximal $F_a=21.3$ N (at $\varphi=(5/9)\pi$).

Table 4 Measurements of the ultimate position of the object where a pinch grasp could be established (Y_{pinch}), the ultimate position, which resulted in a stable power grasp (Y_{pull}), and the final equilibrium position of the power grasp (Y_{power}) of objects with a diameter (*D*) of 80 and 130 mm, with (*f*) and without (*nf*) friction between the object and finger. Values between brackets denote the standard deviation.

D (mm)	Y_{pinch} (mm)	Y_{pull} (mm)	Y_{power} (mm)
80 (*nf*)	158.2(1.5)	153.2(0.8)	<35
80 (*f*)	165.2(0.5)	137.4(0.9)	<35
130 (*nf*)	147.4(1.5)	137.4(1.1)	65.4 (0.5)
130 (*f*)	170.0(0.9)	123.4(0.9)	66.6 (0.5)

4.2 Preliminary Experiments. Preliminary experiments were performed to determine the accuracy and repeatability of the experiments and to show typical results, which can be obtained with this platform. The ability to grasp and the ability to hold objects with a diameter of 80 mm and 130 mm were assessed. Both experiments were repeatedly performed ($N=5$) for frictionless and frictional contact between the finger and the object. The friction coefficient μ between the acrylic objects and aluminum phalanges was $\mu=0.19$ ($\sigma=8.7\times10^{-3}$).

For the experiments assessing the ability to grasp, the initial position of the prismatic joint of the finger was at 51 mm from the line of symmetry, while a linear spring of stiffness $k_x=4.71$ N/mm was applied between the slider and the fixed world. On the proximal and distal joint, torsional springs were mounted of stiffness $k_{\vartheta_1}=15.5$ and $k_{\vartheta_2}=11.5$ N mm rad^{-1} and of an initial angle $\vartheta_1=(13/36)\pi$ and $\vartheta_2=-(2/36)\pi$, respectively. The initial position of the object was progressively moved toward the finger mechanism with steps of 1 mm. For each step, the actuation force of the finger was manually increased from 0 N to 22 N (i.e., approximately the normal actuation force of the finger in this setup). This was continued until the first position was found where the finger could obtain grasp equilibrium with only the distal phalanx (pinch grasp), and second, until the position was found where the finger started to pull the object inside the hand and obtained grasp equilibrium with both phalanges (power grasp). Table 4 shows the measured ultimate position of the object where the pinch grasp was established (Y_{pinch}), the ultimate position, which resulted in a stable power grasp (Y_{pull}), and the final equilibrium position of the power grasp (Y_{power}). Due to friction in the linear guide, we observed a range of positions where the object was neither pulled into the hand nor ejected out of the hand, but remained grasped by the distal phalanx only (pinch grasp). This range increased for the experiment with friction between the object and finger.

For the experiments assessing the ability to hold, we used the same stiffnesses and initial positions of the joints as in the previous experiment that assessed the ability to hold. The mean force in the actuation cable during all experiments was 23.3 N. The object of 80 mm and 130 mm diameter was pulled out of the hand, starting from an initial position of 44 mm and 60 mm, respectively, and ending at a position where the finger was reconfigured to a straight configuration (i.e., $\vartheta_2=0$). The unfiltered results of all repeated measurements are shown in Fig. 7. In this graph, the measured displacement force is normalized relative to the mean actuation force. Two equilibrium points are marked at the fourth data set in this figure. The first equilibrium point denotes the stable power grasp, while the second point is the unstable pinch grasp. For the experiments with friction between the object and the finger, stick-slip behavior was observed, causing more variance in the measurements.

To obtain the mean force-displacement characteristics, the data was resampled using the spline.m in MATLAB and interpolated at a constant displacement step of 0.1 mm (18 Hz). Then for each sample point, the mean and standard deviation is calculated. The median of the standard deviation of all sample points for the experiments without (*nf*) and with (*f*) friction between the finger and the object of 80 mm and 130 mm are $\sigma_{nf80}=0.10$ N, $\sigma_{f80}=0.57$ N, $\sigma_{nf130}=0.09$ N, and $\sigma_{f130}=0.51$ N, respectively.

5 Discussion

In order to assess the ability to grasp and hold objects by underactuated hands and to validate grasp models that predict this

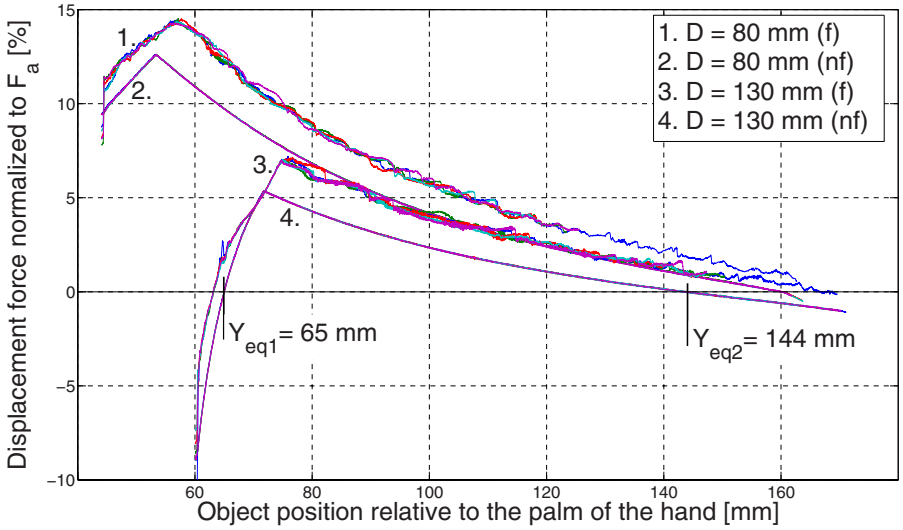

Fig. 7 Measured forces to displace the object all the way out of the hand, where the repetitive measurements are shown on top of each other by different colors. The force is expressed as percentage of the actuation force of the finger. *D* denotes the object diameter, while (*f*) and (*nf*) denotes contact with and without friction, respectively. For experiment 4, the equilibrium positions Y_{eq_1} (stable power grasp) and Y_{eq_2} (unstable pinch grasp) are identified.

performance, a new platform was created and evaluated in this paper. Preliminary experiments were performed to assess the repeatability.

In Sec. 2, we determined to measure the range of object positions from where they can be successfully grasped with a precision of 3 mm. The results in Table 4 shows that the standard deviation of this experiment can be up to 1.5 mm. The required precision is thus achieved. We assume that the variance is mainly caused by the friction in the linear guide. The resultant of the contact forces directed toward the palm of the hand is almost zero at the edge of the successful grasp range. So, friction in the linear guide is then dominant. The static friction of this linear guide had a large variation, probably caused by dirt. In the preliminary experiments, a significant difference between grasping with and without contact friction was demonstrated. Contact friction decreases the range of positions where an object is pulled into a stable power grasp, while the range where the object is grasped in a pinch grasp is increased.

The validity of the pulling force-displacement measurement is determined by the accuracy and precision of the displacement and force measurement. According to the evaluation results, the displacement can be determined with a precision of 0.5 mm. The preliminary experiments showed a precision (2σ) in the force measurement of 0.2 N for grasping without contact friction, which is 4% of the full scale. For the measurements with contact friction between the acrylic object and aluminum finger, the precision is worse, due to the variation in this friction. In addition, the evaluation of the load cell showed a maximum systematic error of +0.1 N, due to contact forces in the direction parallel to the leaf springs and a bending moment about the vertical axis. However, the magnitude of these forces and moments can be predicted by the grasp model, as briefly introduced in Sec. 1. So, it is possible to correct the measured force and eliminate this systematic error.

The experiments on this platform are a first step toward functional benchmark tests for evaluation and optimization of underactuated or compliant robotic hands. In our opinion, the limitation to planar, symmetrical grasps with objects moving along the line of symmetry resulted in an easily repeatable experiment, while the effect of design parameters of the hand on its performance can already be investigated. However, when pulling the object in other directions or pulling without constraining the object motion, the maximum permitted force might be less. Also, when dynamics are considered in the experiments, the performance can be affected. In the tradeoff between more complicated experiments and potentially more accurate results, initially, the simplest and clearest was chosen. Future research must show if more complicated experiments are needed for a more effective and accurate design evaluation and optimization.

6 Conclusions

The performance of planar, symmetrical grasps by compliant or underactuated fingers can be experimentally assessed with the platform developed and described in this paper. An effective way to measure frictionless grasping of cylindrical objects was achieved by using objects consisting of separate disks that can independently rotate about the same vertical axis. If there are as many disks as there are phalanges, and if each disk can make contact with one phalanx only, the object rolls—instead of slips—along the phalanges.

The range of initial object positions where it can be successfully grasped is measured on this platform with a precision of 3 mm. This measurement addresses the ability of robotic hands to grasp objects, while the initial pose of the object is uncertain. In addition, the force required to displace a grasped object all the way out of the hand along the line of symmetry is measured with a precision of 0.2 N for cylindrical objects without contact friction. This measurement addresses the ability to hold grasped objects while they are subject to disturbances. The experiments on this platform can be considered as benchmark tests to compare and optimize the performance of compliant or underactuated robotic hands of arbitrary scale or architecture.

Acknowledgment

This work was carried out as part of the FALCON project under the responsibility of the Embedded Systems Institute with Vanderlande Industries as the industrial partner. This project is partially supported by the Dutch Ministry of Economic Affairs under the Embedded Systems Institute program (Grant No. BSIK03021).

We thank Jan van Frankenhuyzen and Jos van Driel for their advice regarding the mechanical and electrical design aspects of the experimental setup. Anglepoise Ltd. is gratefully acknowledged for providing the zero-free-length spring.

References

[1] Birglen, L., Laliberté, T., and Gosselin, C. M., 2008, "Underactuated Robotic Hands," *Springer Tracts in Advanced Robotics*, Springer-Verlag, Berlin, Vol. 40.

[2] Bicchi, A., 2000, "Hands for Dexterous Manipulation and Robust Grasping: A Difficult Road Toward Simplicity," IEEE Trans. Rob. Autom., **16**(6), pp. 652–662.

[3] Zollo, L., Roccella, S., Guglielmelli, E., Carrozza, M., and Dario, P., 2007, "Biomechatronic Design and Control of an Anthropomorphic Artificial Hand for Prosthetic and Robotic Applications," IEEE/ASME Trans. Mechatron., **12**(4), pp. 418–429.

[4] Hirose, S., and Umetani, Y., 1978, "The Development of Soft Gripper for the Versatile Robot Hand," Mech. Mach. Theory, **13**, pp. 351–359.

[5] Montambault, S., and Gosselin, C. M., 2001, "Analysis of Underactuated Mechanical Grippers," J. Mech. Des., **123**(3), pp. 367–374.

[6] Birglen, L., and Gosselin, C. M., 2006, "Geometric Design of Three-Phalanx Underactuated Fingers," J. Mech. Des., **128**, pp. 356–364.

[7] Dollar, A. M., and Howe, R. D., 2005, "Towards Grasping in Unstructured Environments: Grasper Compliance and Configuration Optimization," Adv. Rob., **19**(5), pp. 523–543.

[8] Kamikawa, Y., and Maeno, T., 2008, "Underactuated Five-Finger Prosthetic Hand Inspired by Grasping Force Distribution of Humans," *Proceedings of the 2008 IEEE/RSJ International Conference on Intelligent Robots and Systems*, pp. 717–722.

[9] Kragten, G. A., and Herder, J. L., "The Ability of Underactuated Hands to Grasp and Hold Objects," Mech. Mach. Theory, **45**, pp. 408–425.

[10] Kragten, G. A., Kool, A. C., and Herder, J. L., 2009, "Ability to Hold Grasped Objects by Underactuated Hands: Performance Prediction and Experiments," *Proceedings of the 2009 IEEE International Conference on Robotics and Automation*, pp. 2493–2498.

[11] European Robotics Research Network (EURON), "Benchmarking Initiative: Manipulation and Grasping," http://www.euron.org/activities/benchmarks/grasping

[12] Kragten, G. A., Bosch, A. H., van Dam, T., Slobbe, J. A., and Herder, J. L., 2009, "On the Effect of Contact Friction and Contact Compliance on the Grasp Performance of Underactuated Hands," ASME Paper No. DETC2009-86541.

[13] Carwardine, G., 1932, "Improvements in Elastic Force Mechanisms," Specifications of Inventions, Patent Office Sale Branch, London, UK Patent No. 379.680.